communications physics

ARTICLE

https://doi.org/10.1038/s42005-022-01050-7 OPEN

Emergence and manipulation of non-equilibrium Yu-Shiba-Rusinov states

Jasmin Bedow [1], Eric Mascot [1,2] & Dirk K. Morr [1✉]

The experimental advances in the study of time-dependent phenomena has opened a new path to investigating the complex electronic structure of strongly correlated and topological materials. Yu-Shiba-Rusinov (YSR) states induced by magnetic impurities in *s*-wave superconductors provide an ideal candidate system to study the response of a system to time-dependent manipulations of the magnetic environment. Here, we show that by imposing a time-dependent change in the magnetic exchange coupling, by changing the relative alignment of magnetic moments in an impurity dimer, or through a periodic drive of the impurity moment, one can tune the system through a time-dependent quantum phase transition, in which the system undergoes a transition from a singlet to a doublet ground state. We show that the electronic response of the system to external perturbations can be imaged through the time-dependent differential conductance, $dI(t)/dV$, which, in analogy to the equilibrium case, is proportional to a non-equilibrium local density of states. Our results open the path to visualizing the response of complex quantum systems to time-dependent external perturbations.

[1] Department of Physics, University of Illinois at Chicago, Chicago, IL 60607, USA. [2] Present address: School of Physics, University of Melbourne, Parkville, VIC 3010, Australia. ✉email: dkmorr@uic.edu

The experimental ability to probe and manipulate complex electronic correlations at the femtosecond time scale has opened unprecedented opportunities for the study of non-equilibrium quantum phenomena in strongly correlated or topological materials[1–5]. The development of next-generation spintronics and quantum computing applications requires the control of magnetic environments not only on similar time scales, but also on nanoscopic length scales. The latter has been achieved by using scanning tunneling spectroscopy (STS) techniques that have enabled the writing of magnetic skyrmions[6], the tuning of local magnetic exchange couplings[7–9], and, in combination with electron spin resonance (ESR) techniques, the rotation of individual magnetic moments in impurity clusters[10]. These techniques were successfully applied[9] to tune the energy of Yu–Shiba–Rusinov (YSR) states[11–13]—induced by magnetic impurities placed on the surface of an *s*-wave superconductor—and thus to drive the system through a quantum phase transition[14–17]. While the required control of magnetic environments on electronic time scales has yet to be achieved, recent progress[10] has raised the question not only of how quantum phenomena—such as quantum phase transitions—can be manipulated on the (electronic) femtosecond or picosecond time scale, but also of how such time-dependent phenomena can be described theoretically and visualized experimentally.

In this article, we address this question by investigating the manipulation of YSR states[11–13] on electronic time scales. By using two different theoretical methods based on the non-equilibrium Keldysh formalism[18–20] we study the non-equilibrium emergence and manipulation of YSR states in response to external perturbations of the magnetic environment. We show that the time evolution of YSR states can be visualized through the time-dependent differential conductance, $dI(t)/dV$, which, in analogy to the equilibrium case, is proportional to a non-equilibrium local density of states (LDOS), N_{neq}. These findings allow us to study the time-dependent phase transition of the system from a singlet to a doublet ground state by subjecting it to a time-dependent change in either the strength of a magnetic impurity's exchange coupling, or in the relative orientation of moments in a magnetic dimer, or by externally driving a periodic precession of an impurity's magnetic moment. Moreover, we show that the extent to which the system is driven out-of-equilibrium is controlled by the time scale over which perturbations occur, and is directly reflected in the time and frequency dependence of N_{neq}. Finally, our formalism reveals the transient behavior between static and periodically driven magnetic structures, allowing us to visualize the emergence of Floquet YSR states[21–23]. Our work thus provides a theoretical framework to study the emergence of non-equilibrium phenomena on electronic time and nanoscopic length scales in complex materials.

Results

Theoretical method. To study the non-equilibrium emergence and manipulation of YSR states, we consider magnetic impurities that are placed on the surface of an *s*-wave superconductor, with the exchange coupling or orientation of magnetic moments being time-dependent. Such a system is described by the Hamiltonian $\mathcal{H} = \mathcal{H}_0 + \mathcal{U}(t)$, where

$$\begin{aligned}\mathcal{H}_0 =& -t_e \sum_{\langle \mathbf{r},\mathbf{r}'\rangle,\sigma} c^\dagger_{\mathbf{r},\sigma} c_{\mathbf{r}',\sigma} - \mu \sum_{\mathbf{r}} c^\dagger_{\mathbf{r},\sigma} c_{\mathbf{r},\sigma} \\ &+ \Delta_0 \sum_{\mathbf{r}} \left(c^\dagger_{\mathbf{r},\uparrow} c^\dagger_{\mathbf{r},\downarrow} + h.c. \right), \\ \mathcal{U}(t) =& J(t) \sum_{\mathbf{R},\alpha,\beta} c^\dagger_{\mathbf{R},\alpha} \left[\mathbf{S}_{\mathbf{R}}(t) \cdot \boldsymbol{\sigma} \right]_{\alpha\beta} c_{\mathbf{R},\beta},\end{aligned} \tag{1}$$

where $-t_e$ is the nearest-neighbor hopping parameter on a square lattice, μ is the chemical potential, Δ_0 is the superconducting *s*-wave order parameter, and $c^\dagger_{\mathbf{r},\sigma}$ creates an electron with spin σ at site $\mathbf{r}$. J is the magnetic exchange coupling and $\mathbf{S}_{\mathbf{R}}$ is the impurity spin at site $\mathbf{R}$ with the last sum running over all impurity positions. Since the hard superconducting *s*-wave gap suppresses Kondo screening[17,24], we take the magnetic impurity spin as classical in nature[17], i.e., $\mathbf{S}_{\mathbf{r}} = S(\sin\theta\cos\phi, \sin\theta\sin\phi, \cos\theta)$, where θ and ϕ are the polar and azimuthal angles, respectively. Finally, we note that the perturbation $\mathcal{U}(t)$ is purely magnetic in nature, and thus does not break particle–hole symmetry.

To theoretically study the electronic response of the system to a time-dependent J or $\mathbf{S}_{\mathbf{r}}$, we recall that the primary experimental probe in the study of YSR states is the differential conductance, dI/dV, measured in STS experiments[17]. We therefore compute the time-dependent current flowing between an STS tip and the superconductor using a formulation of the non-equilibrium Keldysh formalism in the interaction representation[18,19,25], yielding

$$I(V,t) = \frac{e}{\hbar}(-t_{\mathrm{tun}}) \sum_{\sigma} \left[G^<_{ts}(\sigma,t,t) - G^<_{st}(\sigma,t,t) \right], \tag{2}$$

where t_{tun} is the tunneling amplitude between the tip and the superconductor, V is the applied bias, and $G^<_{ts}$ is the spin-dependent, equal-time lesser Green's function between the tip (t) and the site in the superconductor (s) that the electrons tunnel into[25]. Due to the picometer spatial resolution achieved in STS experiments[26], we here assume that the electrons tunnel into a single site of the superconductor only. To compute $G^<_{ts}$, we employ the Keldysh Dyson equations in real time, given by

$$\begin{aligned}\bar{G}^<_{ts}(t,t) =& \bar{g}^<_{ts}(t,t) + \int dt_1 \bar{g}^{\mathrm{r}}_{ts}(t,t_1)\bar{\mathcal{U}}(t_1)\bar{G}^<_{ss}(t_1,t) \\ &+ \int dt_1 \bar{g}^<_{ts}(t,t_1)\bar{\mathcal{U}}(t_1)\bar{G}^{\mathrm{a}}_{ss}(t_1,t) \\ \bar{G}^{\mathrm{a}}_{ts}(t',t) =& \bar{g}^{\mathrm{a}}_{ts}(t',t) + \int dt_1 \bar{g}^{\mathrm{a}}_{ts}(t',t_1)\bar{\mathcal{U}}(t_1)\bar{G}^{\mathrm{a}}_{ss}(t_1,t),\end{aligned} \tag{3}$$

where $\bar{g}^{<,r,a}$ are the equilibrium lesser, retarded and advanced Greens function matrices of the unperturbed system in Nambu space, and $\bar{\mathcal{U}}(t)$ is the time-dependent perturbation matrix arising from Eq. (1). By discretizing time, Eq. (3) transforms into a set of coupled matrix equations, allowing us to obtain a closed form for $G^<_{ts}(t,t)$ (for details, see Supplementary Note 1). Below all times are given in units of $\tau_e = \hbar/t_e$ which implies that for typical values of t_e of a few hundred meV, τ_e is of the order of a few femtoseconds.

As the calculation of dI/dV using Eq. (2) is computationally intensive, we also employ an alternative, computationally more efficient approach using the Heisenberg representation of the Keldysh formalism[19,20]. This approach utilizes the fact that in equilibrium, the differential conductance is proportional to the local density of states $N(\mathbf{r},\omega) = -\mathrm{Im}\, g^{\mathrm{r}}(\mathbf{r},\mathbf{r},\omega)/\pi$. To define an analogous quantity out-of-equilibrium, we note that in the presence of a time-dependent perturbation, $G^{\mathrm{r}}(t,t')$ depends explicitly on t and t'. Setting $t' = t - \Delta t$ and performing a Fourier transformation with regards to Δt, we obtain a time and frequency dependent Greens function $G^{\mathrm{r}}(t,\omega)$, allowing us to define a "non-equilibrium" density of states, N_{neq}, via

$$N_{\mathrm{neq}}(\mathbf{r},\sigma,t,\omega) = -\frac{1}{\pi}\mathrm{Im}G^{\mathrm{r}}(\mathbf{r},\mathbf{r},\sigma,t,\omega), \tag{4}$$

where $G^{\mathrm{r}}(t,\omega)$ is obtained from

$$\left[i\frac{d}{dt} + \omega + i\Gamma - \hat{H}(t) \right] \hat{G}^{\mathrm{r}}(t,\omega) = \hat{1}, \tag{5}$$

for an arbitrary time dependence of the Hamiltonian. Here, $\hat{H}(t)$, $\hat{G}^{\mathrm{r}}(t,\omega)$ and $\hat{1}$ are matrices in real and Nambu space (for details,

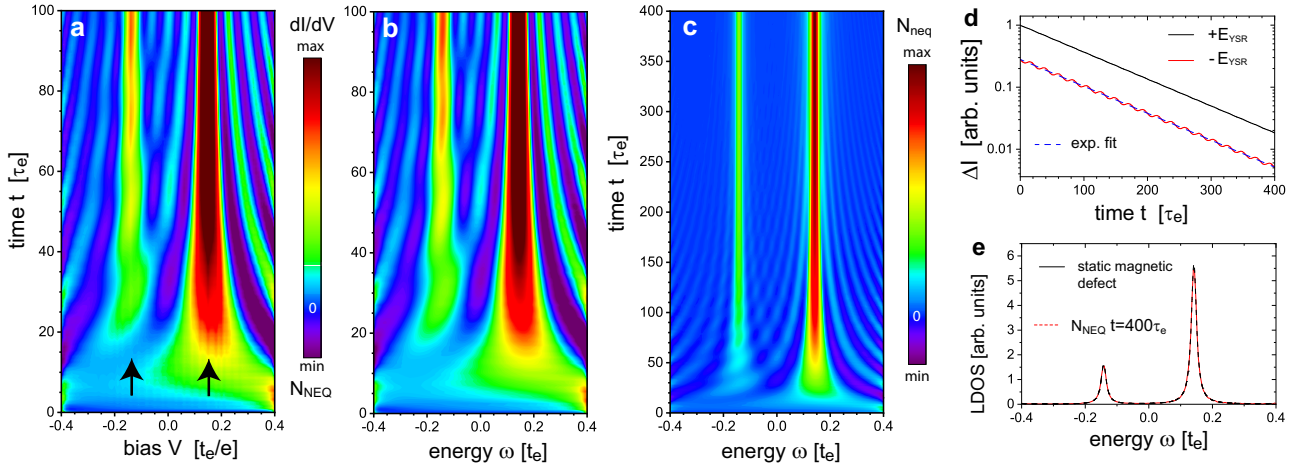

Fig. 1 Non-Equilibrium Emergence of Yu-Shiba-Rusinov States. Time evolution of **a** the differential conductance dI/dV, and **b**, **c** the non-equilibrium local density of states $N_{neq}(\mathbf{r}, t, \omega)$ at the site of the magnetic impurity (we set $\hbar = 1$ such that ω has the units of energy). The colorbar in **a** represents the normalized dI/dV, the colorbar next to **c** represents the normalized N_{neq} in **b**, **c**. **d** Time evolution of the deviation of the Yu–Shiba–Rusinov (YSR) peaks' height from equilibrium, ΔI, as obtained from N_{neq} in **c**. **e** Comparison of the equilibrium local density of states (LDOS) in the presence of a magnetic impurity, and $N_{neq}(\mathbf{r}, t, \omega)$ at $t = 400\tau_e$. Here, $\tau_e = \hbar/t_e$ with the nearest-neighbor hopping parameter $-t_e$. The calculation of dI/dV and N_{neq} used identical parameters sets with $(\mu, JS, \Delta_0) = (-2.0, 1.8, 0.4)t_e$, and $\Gamma = 0.01t_e$. Here, μ is the chemical potential, J is the magnetic coupling, S is the spin of the adatoms and Δ_0 is the superconducting order parameter. For the calculation of dI/dV, we used $t_{tun} = 0.01t_e$ for the tunneling between the system and the tip, corresponding to the weak-tunneling limit. The same parameters are also used in the following figures. The results for N_{neq} were obtained for a 50×50 site real space system.

see Supplementary Note 2), and $\tau_\Gamma = \hbar/\Gamma$ is the quasi-particle lifetime[17]. We demonstrate below that N_{neq} is proportional to the time-dependent $dI(V,t)/dV$, and thus represents a physical observable that describes the non-equilibrium time evolution of the superconductor's electronic structure.

Non-equilibrium emergence of YSR states. We begin by considering the question of how a YSR state emerges when a single magnetic impurity is placed on the surface of an *s*-wave superconductor at time $t = 0$. To this end, we consider a perturbation of the form

$$\mathcal{U}(t \geq 0) = JS \sum_{\alpha,\beta} c^\dagger_{\mathbf{r},\alpha} \sigma^z_{\alpha\beta} c_{\mathbf{r},\beta}, \tag{6}$$

where S is the magnitude of the impurity spin, and $\mathcal{U}(t < 0) = 0$. In Fig. 1a, we present the resulting time and bias dependence of $dI(V,t)/dV$ as obtained from Eq. (2) (due to the significant computational resources required, the calculation of dI/dV is limited to $t \leq 100\tau_e$). At $t = 0$, the LDOS is that of an unperturbed *s*-wave superconductor without a magnetic impurity, exhibiting a hard gap and coherence peaks at $\pm\Delta_0$. As the magnetic impurity is placed on the surface, spectroscopic weight from the gap edges begins to be transferred into the gap, creating at first a broad peak centered around the energy of the emerging YSR state (see black arrows in Fig. 1a). This shift of spectroscopic weight occurs in a wave-like form, as reflected in the stripe-like patterns of $dI(V,t)/dV$ in Fig. 1a[27,28]. With increasing time, the width of the peaks decreases, while their height increases, which is a direct consequence of the uncertainty principle: $t\Delta E \geq \hbar$ implies that as the time over which the impurity is located on the surface increases, the YSR state's energy uncertainty, i.e., the peaks' width, decreases.

To elucidate the relation between dI/dV and N_{neq}, we note that for the perturbation of Eq. (6), the solution of Eq. (5) is given by

$$\begin{aligned}\hat{G}^r(t,\omega) = &\left[1 - e^{i\left(\omega\hat{1} - \hat{H}^+\right)t} e^{-\Gamma t}\right] \hat{g}^r_+(\omega) \\ &+ e^{i\left(\omega\hat{1} - \hat{H}^+\right)t} e^{-\Gamma t} \hat{g}^r_0(\omega)\end{aligned} \tag{7}$$

where $\hat{g}^r_{0,+}$ are the equilibrium Green's functions for a system without and with an impurity, respectively, and $\hat{H}^+$ is the full Hamiltonian for $t \geq 0$. We thus have $\hat{G}^r(t = 0, \omega) = \hat{g}^r_0(\omega)$ and $\hat{G}^r(t \to \infty, \omega) = \hat{g}^r_+(\omega)$. A comparison of N_{neq} obtained from Eqs. (4) and (7) (see Fig. 1b) with dI/dV (see Fig. 1a) shows remarkable quantitative agreement (up to an overall scaling factor) in the (ω, t)-plane (a more detailed comparison is provided in Supplementary Movie 1). This suggests that $dI(V,t)/dV \sim N_{neq}(t, \omega = eV)$, implying that N_{neq} represents a physical observable that describes the non-equilibrium time evolution of the superconductor's electronic structure. Since N_{neq} is computed in the absence of a tip, we expect $dI/dV \sim N_{neq}$ to hold only in the weak-tunneling regime, similar to the equilibrium case[17]. As the calculation of N_{neq} is computationally less demanding than that of dI/dV, we can now study the time-evolution of the system up to much larger times using N_{neq}, as shown in Fig. 1c, where we present $N_{neq}(t, \omega)$ up to $t = 400\tau_e$. Eq. (7) suggests that when $\omega = \pm E_{YSR}$, with E_{YSR} being the YSR state energy, the oscillatory term, $\sim e^{i\left(\omega\hat{1} - \hat{H}^+\right)t}$ is identical to one, and N_{neq} relaxes exponentially to the static case for $t \to \infty$, with the relaxation time given by τ_Γ[28], which is identical to the lifetime of the YSR state. This is confirmed by a log-plot of the deviation of the YSR peaks' height from the equilibrium value, ΔI, as obtained from N_{neq} in Fig. 1c, as a function of time presented in Fig. 1d, where the dashed line corresponds to $\sim e^{-\Gamma t/\hbar}$. Finally, a comparison of the equilibrium LDOS in the presence of a static magnetic impurity with $N_{neq}(t, \omega)$ at $t = 400\tau_e$ (see Fig. 1e) shows very good agreement, demonstrating that this formalism allows us to study the system during the entire equilibration process. We note that the agreement between dI/dV and N_{neq} is independent of the specific value of Γ chosen (see Supplementary Movie 2), as Γ only controls the relaxation time of the process. Moreover, for more realistic parameters sets, the relaxational dynamics discussed above can be observed on time scales up to 100 ps (see Supplementary Fig. 1).

Dynamical tuning of quantum phase transitions. An intriguing phenomenon associated with the presence of a magnetic impurity

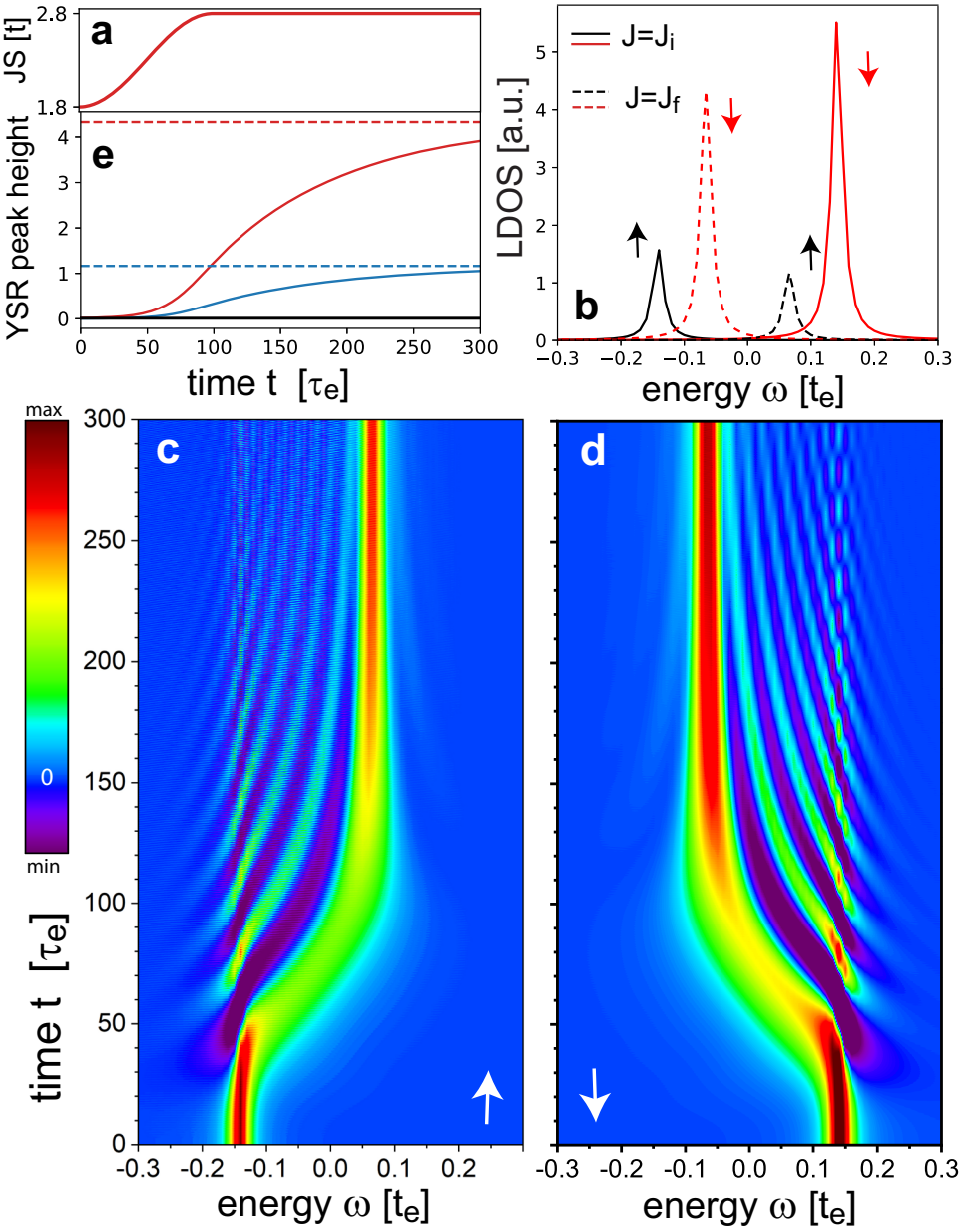

Fig. 2 Dynamical tuning of quantum phase transitions. a Time dependence of the magnetic coupling $J(t)$ with an initial value of $J_i = 1.8t_e < J_c$, a final value of $J_f = 2.8t_e > J_c$, where a quantum phase transition occurs at the critical magnetic coupling of $J_c = 2.45t_e$, and the transition from J_i to J_f occurs over the time $\Delta t = 100\tau_e$. **b** Spin-resolved equilibrium local density of states (LDOS) in the presence of a single magnetic impurity with $J_i < J_c$ and $J_f > J_c$. Time dependence of the spin-resolved non-equilibrium local density of states $N_{neq}(\sigma, t, \omega)$ for **c** spin $\sigma = \uparrow$, and **d** $\sigma = \downarrow$ arising from $J(t)$ in **a**. The colorbar represents the normalized N_{neq}. **e** Height of the Yu–Shiba–Rusinov (YSR) peaks as a function of time, representing the relaxation of the system. The results for N_{neq} were obtained for a 24 × 24 site real space system.

is the possibility to drive the superconductor through a quantum phase transition between a singlet and doublet ground state by either tuning J through a critical value, $J_c = (\pi N_0 S)^{-1}$,[14–17], where N_0 is the normal state density of states at the Fermi energy, or by changing the distance or relative spin alignment of two or more impurities[29,30]. This phase transition is accompanied by a zero-energy crossing of the YSR peaks in the LDOS. To investigate whether such a phase transition can also be induced using non-equilibrium techniques[31,32], we begin by considering the case of a time-dependent exchange coupling J, which is motivated by the experimental ability to significantly vary J using STS techniques[7–9]. Specifically, we increase the exchange coupling from an initial value $J_i < J_c$ at $t = 0$ to a final value $J_f > J_c$ at a time $t = \Delta t$, using the time evolution $J(t) = J_i + (J_f - J_i)\sin^2\left(\frac{\pi t}{2\Delta t}\right)$ for $0 \le t \le \Delta t$ as shown in Fig. 2a. A plot of the equilibrium LDOS for $J = J_{i,f}$ in Fig. 2b demonstrates that the zero energy crossing of the YSR peaks at the phase transition exchanges the spin projection of their particle- and hole-like branches[14–17], which can be mapped using spin-polarized STS[33]. The time evolution of the phase transition can thus be best visualized by considering the spin-resolved $N_{neq}(\sigma, t, \omega)$, shown in Fig. 2c, d for $\sigma = \uparrow$ and $\sigma = \downarrow$, respectively. While the change in J over a finite time Δt leads to significant oscillations in N_{neq}, a zero-energy crossing of the YSR peaks, indicating a time-dependent phase transition[14–17], can still be identified. Moreover, N_{neq} reveals several noteworthy features. First, the spectral weight of the YSR peaks is decreased

during the zero-energy crossing, concomitant with the phase transition. Second, a substantial redistribution of the YSR state's spectral weight begins to occur only after $t \approx 50\tau_e = \Delta t/2$, indicating a delayed response of the system to the imposed change in J. This is particularly evident from comparison of the time-dependent YSR peak height at the final energy position in Fig. 2e with $J(t)$ shown in Fig. 2a. Third, substantial oscillations in $N_{\rm neq}$ at the energy of the original YSR peaks persist up to time scales significantly longer than Δt, and the spectral weight of these oscillations is shifted to the final energy position of the YSR states in a wave-like pattern, as evidenced by the stripe-like pattern in $N_{\rm neq}$ (see Fig. 2c, d). Finally, a comparison of dI/dV and $N_{\rm neq}$ shown in Supplementary Movie 3 again reveals good quantitative agreement between them, further supporting our conclusion that $dI/dV \sim N_{\rm neq}$.

Twisting a spin dimer. The superconductor can also be tuned through a quantum phase transition by changing the relative alignment of the spins of two impurities in close proximity from antiparallel to parallel[29], even if each of the two impurities possesses an exchange coupling smaller than the critical value, J_c. Such a change in the spins' relative alignment in an impurity dimer has been achieved using ESR techniques[10]. For antiparallel alignment, the YSR states associated with each impurity cannot hybridize as the spin quantum number of their particle- and hole-like branches are opposite. The LDOS thus exhibits two pairs of degenerate YSR states with opposite spin quantum numbers[29], as shown in Fig. 3a, b. When the alignment is rotated to parallel, the YSR states hybridize, leading to an energy splitting between them and the emergence of four peaks in the LDOS (see Fig. 3a, b). Plotting the equilibrium LDOS as a function of the angle θ between the spins (Fig. 3c, d), corresponding to the adiabatic limit of the rotation, we find that the energy splitting increases with decreasing θ, leading to a zero energy crossing of two of the YSR peaks, and a concomitant phase transition from a singlet to a doublet ground state. The question naturally arises as to the time dependence of such a phase transition when the relative alignment is changed over a finite time Δt, as was done in ref. [10] through the application of an ESR π pulse. To address this question, we consider for concreteness the rotation of one of the two impurity spins through the xz plane described by $\mathbf{S}_\mathbf{r} = S[\sin\theta(t), 0, \cos\theta(t)]$, with the time-dependent polar angle given by

$$\theta(t) = \pi \cos^2\left(\frac{\pi}{2\Delta t} t\right), \quad \text{for } 0 \le t \le \Delta t. \tag{8}$$

In Fig. 3e, f we present the resulting spin-resolved $N_{\rm neq}(\sigma, t, \omega)$ for $\Delta t = 200\tau_e$, with the spins being antiparallel for $t = 0$ and parallel for $t = \Delta t$. As before, we can identify a time-dependent zero-energy crossing of the YSR peaks (see yellow arrows in Fig. 3e, f) indicating a phase transition from a singlet to a doublet ground state. We note that the angular dependence of the equilibrium LDOS shown in Fig. 3c, d, corresponds to the time dependence of $N_{\rm neq}$ between $0 \le t \le \Delta t$ (see white dashed line in Fig. 3e, f) in the adiabatic limit of $\Delta t \to \infty$. A comparison of the equilibrium LDOS with $N_{\rm neq}$ in Fig. 3e, f thus reveals that a finite Δt leads to significant time-dependent oscillations in $N_{\rm neq}$, in particular near the energy positions of the YSR peaks at $t = 0$, $\pm E^{(0)}_{\rm YSR}$. To investigate how the strength of these oscillations depends on Δt, we plot in Fig. 3g, h $N_{\rm neq}(t_\Delta, \pm E^{(0)}_{\rm YSR})$ as a function of time after the rotation is completed, i.e., $t_\Delta = t - \Delta t$, for two different values of Δt. We find that the amplitude of the oscillations in $N_{\rm neq}(t_\Delta, \omega)$ increases with decreasing Δt as the system is more strongly driven out of equilibrium. This result is consistent with the expectation that in the quasi-static, adiabatic limit, $\Delta t \to \infty$, these oscillations vanish, and $N_{\rm neq}$ becomes identical to the equilibrium LDOS in Fig. 3c, d, when plotted as a function of angle.

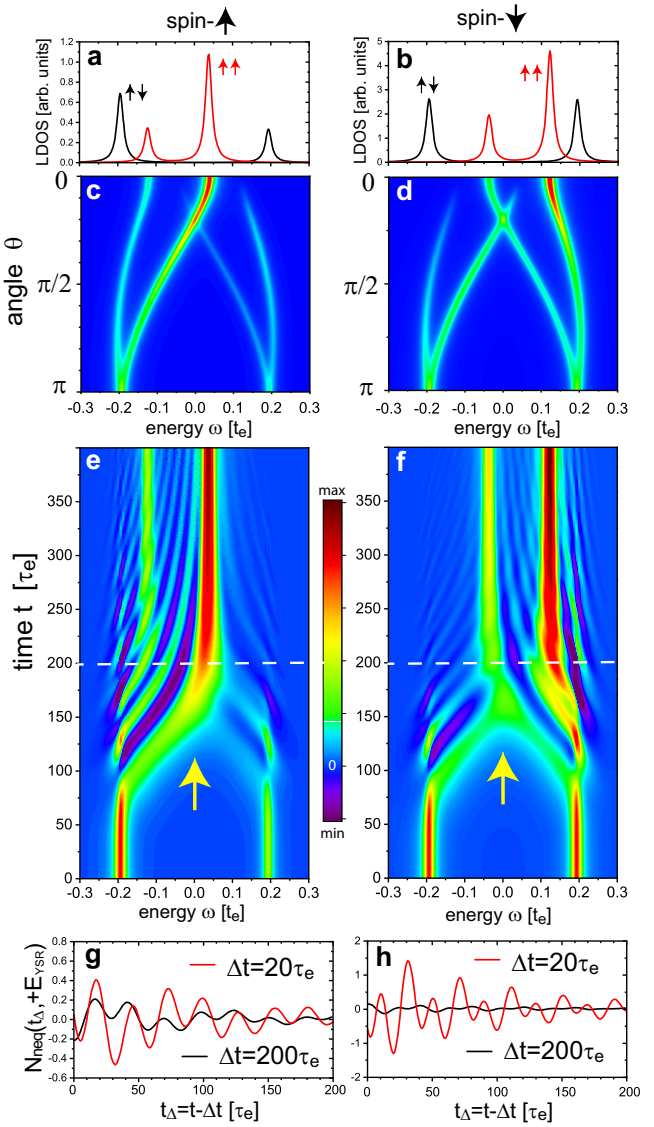

Fig. 3 Twisting a spin dimer. Equilibrium **a** spin-↑ and **b** spin-↓ local density of states (LDOS) for parallel (↑↑) and antiparallel (↑↓) alignment of the spins of two magnetic impurities, located on nearest-neighbor sites. The LDOS is computed at the site of the spin-↑ magnetic impurity. Quasi-static evolution of the **c** spin-↑, **d** spin-↓ LDOS as a function of the angle θ between the two magnetic moments. Spin-resolved non-equilibrium local density of states $N_{\rm neq}(\sigma, t, \omega)$ for **e** $\sigma = \uparrow$, and **f** $\sigma = \downarrow$ arising from the relative rotation of the impurity moments. The colorbar represents the normalized $N_{\rm neq}$. $N_{\rm neq}(\sigma, t_\Delta, \omega)$ for **g** $\sigma = \uparrow$, and **h** $\sigma = \downarrow$ as a function of the time after the perturbation t_Δ (see text). The results for $N_{\rm neq}$ were obtained for a 24 × 24 site real space system.

Emergence of Floquet YSR states. The formalism presented above can also be employed to investigate periodically driven systems, which are typically studied using the Floquet formalism[21–23], and the transient behavior of quantum systems between the static and periodically driven limits. The latter is of particular interest since heating effects in interacting systems[34] could potentially destroy novel quantum states, such as Floquet topological insulators[22] or Floquet topological superconductors[35] even before

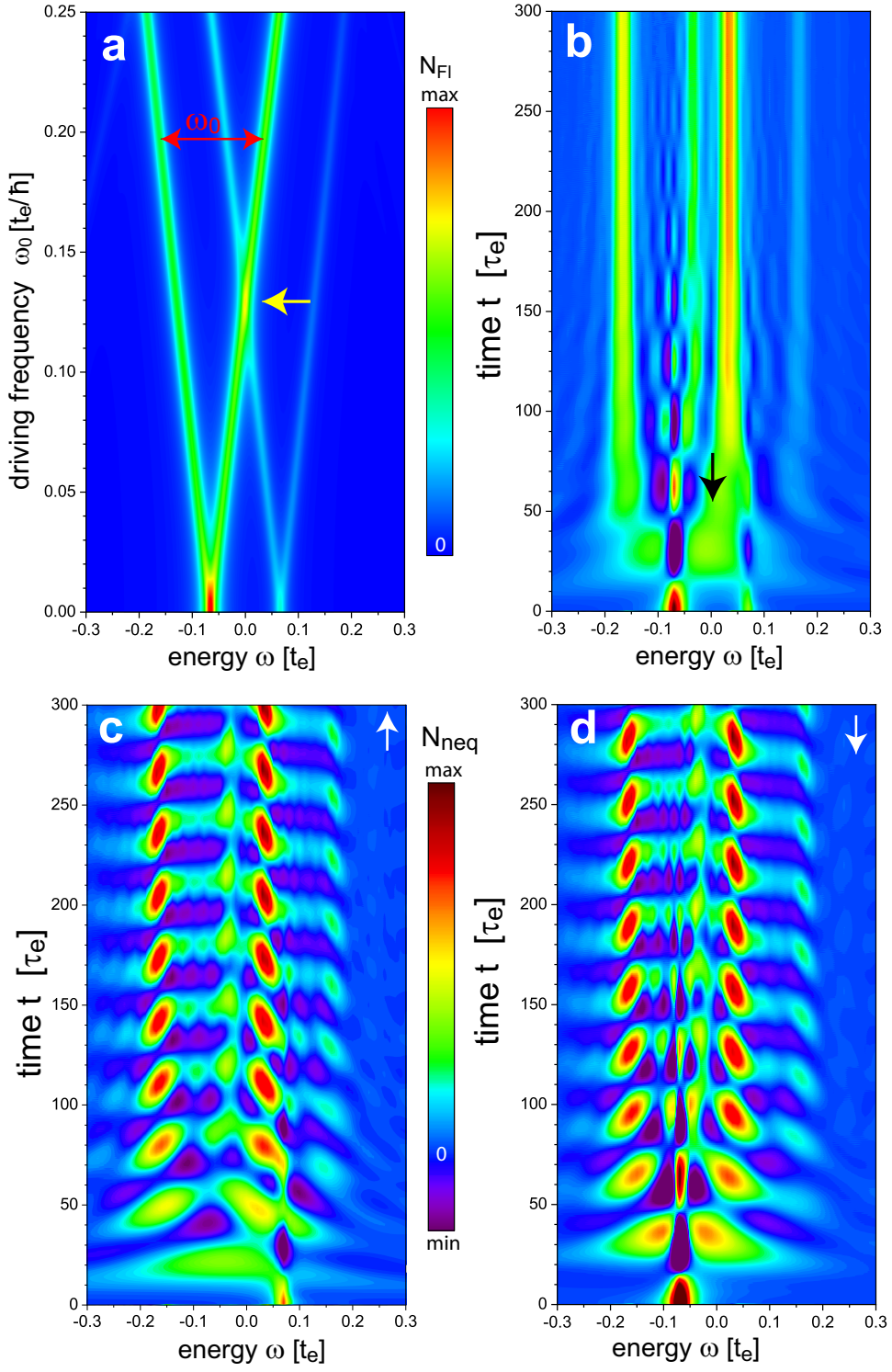

Fig. 4 Emergence of Floquet Yu-Shiba-Rusinov States. a Floquet local density of states (LDOS) N_{FI} as a function of energy for a continuously rotating spin with driving frequency ω_0, with $l = 2$ as the cutoff in the Floquet–Sambe matrix. Note that the energy splitting of the Yu–Shiba–Rusinov (YSR) states (see red arrow) is given by ω_0. The colorbar represents the normalized Floquet LDOS. Time evolution of **b** the non-equilibrium local density of states $N_{neq}(t, \omega)$ summed over both spin orientations, and **c** the spin-resolved $N_{neq}(\uparrow, t, \omega)$ and **d** $N_{neq}(\downarrow, t, \omega)$ for $\omega_0 = 0.2t_e/\hbar$, corresponding to $T = 10\pi\tau_e$. The colorbar next to **c** represents the normalized N_{neq} in **b**–**d**. Here, the magnetic coupling $J = 2.8t_e > J_c$ is larger than the critical value J_c, where a phase transition occurs. The results for N_{neq} were obtained for a 24 × 24 site real space system.

they are fully formed. To study such transient behavior, we consider the case of a single magnetic impurity, and study the time evolution from a single static impurity spin at $t = 0$ to an impurity spin that rotates periodically in the xz-plane with a driving frequency of $\omega_0 = 2\pi/T$. We note that the periodic rotation of the impurity's spin leads to a splitting of the (static) YSR peaks in the density of states[36], with the splitting given by ω_0. This is shown in Fig. 4a where we present the evolution of the Floquet LDOS N_{FI} with increasing driving frequency ω_0 (for details, see Supplementary Note 3). Since, $J = 2.8t_e > J_c$, and since for $\omega \to \infty$ the YSR states

merge with the continuum, as the scattered electrons see a vanishing effective J, a zero-energy crossing of the YSR peaks in N_{Fl} occurs at some critical value of the driving frequency, ω_c, indicating a phase transition (see yellow arrow in Fig. 4a) from a doublet to a singlet ground state. To investigate the transient behavior from a static to a periodically rotating impurity spin, we employ a time-dependent polar angle given by $\theta(t) = \omega_0 t \tanh\left(5\omega_0 t/\pi\right)$ for $0 \le t \le T/2$ and $\theta(t) = \omega_0 t$ for $t \ge T/2$. The resulting N_{neq} shown in Fig. 4b for $\omega_0 = 0.2t_e/\hbar$ clearly reveals the emergence of the YSR peak splitting and of four YSR peaks with increasing time. Since $\omega_0 > \omega_c$ and $J > J_c$, we find that with increasing time, there is a substantial transfer of spectral weight across zero energy, indicating a time-dependent phase transition (see black arrow in Fig. 4b). We note that for $t \gg T$, the system is described by a Hamiltonian that is periodic in time, such that N_{neq} is expected to coincide with the Floquet LDOS N_{Fl}. We find that already for $t = 400\tau_e$, N_{neq} is in very good quantitative agreement with N_{Fl} (see Supplementary Fig. 3 and Supplementary Note 4) that supports the validity not only of the non-equilibrium formalism presented above to describe periodically driven systems, but also the definition of N_{neq} as an observable physical quantity. Moreover, we note that while the total, spin-summed $N_{\mathrm{neq}}(t,\omega)$ does not exhibit any signature of the rotation period (consistent with a time-independent total N_{Fl}), the spin-resolved $N_{\mathrm{neq}}(\sigma,t,\omega)$ shown in Fig. 4c, d does, an effect refereed to as micromotion[37,38]. As expected from a rotation of the spin in the xz-plane, we find that N_{neq} for $\sigma = \uparrow$ and $\sigma = \downarrow$ are out of phase, i.e., shifted by half a period T. A comparison of dI/dV and N_{neq} shown in Supplementary Movie 4 again reveals good quantitative agreement between these quantities, further supporting our conclusion that $dI/dV \sim N_{\mathrm{neq}}$. Due to the numerical complexity in computing dI/dV, we were restricted to time scales $t \le 20\tau_e$ for this comparison.

Discussion

The ability to understand the non-equilibrium response of complex quantum systems to external perturbations on electronic (femtosecond) timescales and nanoscopic length scales is crucial not only for advancing our theoretical understanding of these systems, but also for the development of next generation spintronics and quantum computing applications. Here, we have shown that time-dependent manipulations of magnetic impurities—leading to changes in their exchange coupling or relative spin alignment—not only allow us to study the emergence of quantum phenomena, such as the formation of YSR states, but can also give rise to new intriguing phenomena, such as a time-dependent phase transition. Studying and understanding the response of complex quantum system to external perturbations will be crucial for realizing topological quantum gates, and the required braiding of Majorana fermions. Indeed, the formalism we have presented here provides a suitable approach to study the non-equilibrium response of topological superconductors, and in particular Majorana modes[39–41].

One could envision a few different approaches to realizing experiments capable of probing the relaxational dynamics of the quantum phenomena described above. To this end, experiments would have to be performed on the scale of the lifetime τ_Γ of YSR states, which for more realistic parameters (see Supplementary Fig. 1) might extend up to 100ps. For example, ESR/STS techniques could in general be used to rotate magnetic moments (see ref. [10], which is relevant for the case discussed in Fig. 2 of our manuscript) or change the magnetic exchange interaction (see refs. [7–9], relevant for the case of Fig. 3) while simultaneously measuring the differential conductance dI/dV. The time scale for spin-flip processes in ESR/STS experiments is currently on the order of 20 ns[10], but could plausibly be further reduced by factors of 10–100 by increasing local magnetic fields, for example, created by additional magnetic impurities (Lutz, C. P., private communication). Moreover, the quantum state of individual molecules located in a scanning tunneling microscope (STM) cavity can be manipulated using THz irradiation, with the STM measuring the resulting changes using inelastic tunneling spectroscopy[42]. Similarly, it might be possible to use light-spin interactions to induce spin-oscillations on the ps time scale[43] in magnetic atoms located in an STM cavity. Which of these possible experimental approaches will ultimately be successful can only be determined by future work. Finally, we note that in interacting systems (in contrast to the non-interacting system considered here) non-equilibrium perturbations can lead to detrimental heating effects, which are likely more relevant for periodic drives, such as the one considered in Fig. 4, than for the cases discussed in Figs. 1–3. However, it was shown that even for periodic drives, there exists a pre-thermalization regime[44,45] in which non-equilibrium quantum states can be formed before they are destroyed by heating effects at larger time scales[34]. How heating effects and the pre-thermalization regime can be quantum engineered[46] in the context of YSR states is an interesting question for future work.

Methods

In order to obtain the differential conductance, we employ Eq. (2) to calculate the current between the tip and the system for a given set of bias voltages and numerically take the derivative with respect to the bias voltage. The details regarding the calculation of the Green's functions using the Keldysh formalism can be found in Supplementary Note 1. To calculate the non-equilibrium local density of states, we employ Eqs. (4) and (5). The local density of states in the static case is computed by representing the Hamiltonian of Eq. (1) as a matrix in real and Nambu space and using Supplementary Eq. (S31) to calculate the retarded Green's function matrix $\hat{g}^r$, from which the LDOS is obtained as $N(\mathbf{r},\sigma,\omega) = -\mathrm{Im}\left[\hat{g}^r(\mathbf{r},\sigma;\mathbf{r},\sigma,\omega)\right]/\pi$. The Floquet LDOS N_{Fl} is calculated using the Floquet formalism, which is described in Supplementary Note 3.

Data availability

Original data are available at https://doi.org/10.5281/zenodo.7116734.

Code availability

The codes that were employed in this study are available from the authors on reasonable request.

Received: 1 December 2021; Accepted: 19 October 2022;
Published online: 12 November 2022

References

1. Perfetti, L. et al. Time evolution of the electronic structure of 1T - TaS_2 through the insulator-metal transition. *Phys. Rev. Lett.* **97**, 067402 (2006).
2. Schmitt, F. et al. Transient electronic structure and melting of a charge density wave in $TbTe_3$. *Science* **321**, 1649–1652 (2008).
3. Fausti, D. et al. Light-induced superconductivity in a stripe-ordered cuprate. *Science* **331**, 189–191 (2011).
4. Sobota, J. A. et al. Ultrafast optical excitation of a persistent surface-state population in the topological insulator Bi_2Se_3. *Phys. Rev. Lett.* **108**, 117403 (2012).
5. McIver, J. W. et al. Light-induced anomalous Hall effect in graphene. *Nat. Phys.* **16**, 38–41 (2020).
6. Romming, N. et al. Writing and deleting single magnetic skyrmions. *Science* **341**, 636–639 (2013).
7. Farinacci, L. et al. Tuning the coupling of an individual magnetic impurity to a superconductor: quantum phase transition and transport. *Phys. Rev. Lett.* **121**, 196803 (2018).
8. Yang, K. et al. Tuning the exchange bias on a single atom from 1 mT to 10 T. *Phys. Rev. Lett.* **122**, 227203 (2019).
9. Karan, S. et al. Superconducting quantum interference at the atomic scale. *Nat. Phys.* **18**, 893–898 (2022).
10. Yang, K. et al. Coherent spin manipulation of individual atoms on a surface. *Science* **366**, 509–512 (2019).

11. Yu, L. Bound state in superconductors with paramagnetic impurities. *Acta Phys. Sin.* **21**, 75–91 (1965).
12. Shiba, H. Classical spins in superconductors. *Prog. Theor. Phys.* **40**, 435–451 (1968).
13. Rusinov, A. I. On the theory of gapless superconductivity in alloys containing paramagnetic impurities. *J. Exp. Theor. Phys.* **29**, 1101–1106 (1969).
14. Sakurai, A. Comments on superconductors with magnetic impurities. *Prog. Theor. Phys.* **44**, 1472–1476 (1970).
15. Salkola, M. I., Balatsky, A. V. & Schrieffer, J. R. Spectral properties of quasiparticle excitations induced by magnetic moments in superconductors. *Phys. Rev. B* **55**, 12648 (1997).
16. Bazaliy, Y. B. & Jones, B. A. Magnetic impurity in a superconductor: local phase transitions and finite size effects. *J. Appl. Phys.* **87**, 5561–5563 (2000).
17. Balatsky, A. V., Vekhter, I. & Zhu, J.-X. Impurity-induced states in conventional and unconventional superconductors. *Rev. Mod. Phys.* **78**, 373–433 (2006).
18. Keldysh, L. V. Diagram technique for non-equilibrium processes. *Soviet Phys. Jetp* **20**, 1018–1026 (1965).
19. Rammer, J. & Smith, H. Quantum field-theoretical methods in transport theory of metals. *Rev. Mod. Phys.* **58**, 323–359 (1986).
20. Kamenev, A. & Levchenko, A. Keldysh technique and non-linear σ-model: Basic principles and applications. *Adv. Phys.* **58**, 197–319 (2009).
21. Kohler, S., Lehmann, J. & Hänggi, P. Driven quantum transport on the nanoscale. *Phys. Rep.* **406**, 379–443 (2005).
22. Cayssol, J., Dóra, B., Simon, F. & Moessner, R. Floquet topological insulators. *Phys. Status Solidi RRL* **7**, 101–108 (2013).
23. Oka, T. & Kitamura, S. Floquet engineering of quantum materials. *Annu. Rev. Condens. Matter Phys.* **10**, 387–408 (2019).
24. Heinrich, B. W., Pascual, J. I. & Franke, K. J. Single magnetic adsorbates on s -wave superconductors. *Prog. Surf. Sci.* **93**, 1–19 (2018).
25. Caroli, C., Combescot, R., Nozieres, P. & Saint-James, D. Direct calculation of the tunneling current. *J. Phys. C Solid State Phys.* **4**, 916–929 (1971).
26. Hamidian, M. H. et al. Picometer registration of zinc impurity states in $Bi_2Sr_2CaCu_2O_{8+\delta}$ for phase determination in intra-unit-cell Fourier transform STM. *New J. Phys.* **14**, 053017 (2012).
27. Souto, R. S., Martín-Rodero, A. & Yeyati, A. L. Andreev bound states formation and quasiparticle trapping in quench dynamics revealed by time-dependent counting statistics. *Phys. Rev. Lett.* **117**, 267701 (2016).
28. Taranko, R. & Domański, T. Buildup and transient oscillations of Andreev quasiparticles. *Phys. Rev. B* **98**, 075420 (2018).
29. Morr, D. K. & Stavropoulos, N. A. Quantum interference between impurities: creating novel many-body states in *s* -wave superconductors. *Phys. Rev. B* **67**, 020502 (2003).
30. Morr, D. K. & Yoon, J. Impurities, quantum interference, and quantum phase transitions in s -wave superconductors. *Phys. Rev. B* **73**, 224511 (2006).
31. Seoane Souto, R., Feiguin, A. E., Martín-Rodero, A. & Yeyati, A. L. Transient dynamics of a magnetic impurity coupled to superconducting electrodes: exact numerics versus perturbation theory. *Phys. Rev. B* **104**, 214506 (2021).
32. Wrześniewski, K., Weymann, I., Sedlmayr, N. & Domański, T. Dynamical quantum phase transitions in a mesoscopic superconducting system. *Phys. Rev. B* **105**, 094514 (2022).
33. Cornils, L. et al. Spin-resolved spectroscopy of the Yu-Shiba-Rusinov states of individual atoms. *Phys. Rev. Lett.* **119**, 197002 (2017).
34. Weidinger, S. A. & Knap, M. Floquet prethermalization and regimes of heating in a periodically driven, interacting quantum system. *Sci. Rep.* **7**, 45382 (2017).
35. Jiang, L. et al. Majorana fermions in equilibrium and in driven cold-atom quantum wires. *Phys. Rev. Lett.* **106**, 220402 (2011).
36. Kaladzhyan, V., Hoffman, S. & Trif, M. Dynamical Shiba states from precessing magnetic moments in an s -wave superconductor. *Phys. Rev. B* **95**, 195403 (2017).
37. Goldman, N. & Dalibard, J. Periodically driven quantum systems: effective Hamiltonians and engineered gauge fields. *Phys. Rev. X* **4**, 031027 (2014).
38. Desbuquois, R. et al. Controlling the Floquet state population and observing micromotion in a periodically driven two-body quantum system. *Phys. Rev. A* **96**, 053602 (2017).
39. Tuovinen, R., Perfetto, E., van Leeuwen, R., Stefanucci, G. & Sentef, M. A. Distinguishing Majorana zero modes from impurity states through time-resolved transport. *New J. Phys.* **21**, 103038 (2019).
40. Väyrynen, J. I., Pikulin, D. I. & Lutchyn, R. M. Majorana signatures in charge transport through a topological superconducting double-island system. *Phys. Rev. B* **103**, 205427 (2021).
41. Barański, J., Barańska, M., Zienkiewicz, T., Taranko, R. & Domański, T. Dynamical leakage of Majorana mode into side-attached quantum dot. *Phys. Rev. B* **103**, 235416 (2021).
42. Wang, L., Xia, Y. & Ho, W. Atomic-scale quantum sensing based on the ultrafast coherence of an H2 molecule in an STM cavity. *Science* **376**, 401–405 (2022).
43. Kanda, N. et al. The vectorial control of magnetization by light. *Nat Commun* **2**, 362 (2011).
44. Peng, P., Yin, C., Huang, X., Ramanathan, C. & Cappellaro, P. Floquet prethermalization in dipolar spin chains. *Nat. Phys.* **17**, 444–447 (2021).
45. Beatrez, W. et al. Floquet prethermalization with lifetime exceeding 90 s in a bulk hyperpolarized solid. *Phys. Rev. Lett.* **127**, 170603 (2021).
46. Shkedrov, C. et al. Absence of heating in a uniform Fermi gas created by periodic driving. *Phys. Rev. X* **12**, 011041 (2022).

Acknowledgements

The authors would like to thank G. Czap, K.J. Franke, C.P. Lutz, H. Kim, S. Rachel, J. Wiebe, and R. Wiesendanger for stimulating discussions. This work was supported by the U. S. Department of Energy, Office of Science, Basic Energy Sciences, under Award No. DE-FG02-05ER46225.

Author contributions

D.K.M. conceived and supervised the project. J.B. and E.M. performed the theoretical calculations. D.K.M. wrote the manuscript, with contributions from all authors.

Competing interests

The authors declare no competing interests.

Additional information

Supplementary information The online version contains supplementary material available at https://doi.org/10.1038/s42005-022-01050-7.

Correspondence and requests for materials should be addressed to Dirk K. Morr.

Peer review information *Communications Physics* thanks the anonymous reviewers for their contribution to the peer review of this work. Peer reviewer reports are available.

Reprints and permission information is available at http://www.nature.com/reprints

Publisher's note Springer Nature remains neutral with regard to jurisdictional claims in published maps and institutional affiliations.